

1
2
3 **Investigation of the influence of solar activity on Total Electron Content (TEC) at the Koudougou station**
4 **during recurrent geomagnetic activity during solar cycle 24: A detailed analysis**
5
6
7
8
9

10 **Abstract:**

11 The objective of this article is to examine the dependence of total electron content (TEC) on solar activity
12 parameters such as the sunspot number (SN) index, the F10.7 solar radio flux and the EUV flux. Daily, monthly and
13 annual average TEC data, as well as solar indices, were used for the study. TEC observations were made in
14 Koudougou (12°15'N; -2°20'E), Burkina Faso, using a dual-frequency GPS receiver. The working period covers the
15 years 2010 to 2017, focusing on recurring geomagnetic days. To model the variation in TEC as a function of solar
16 parameters, a quadratic fit was used as a model to describe the daily, monthly and annual variation in TEC. Linear
17 and non-linear coefficients were calculated to understand the trends in the variation. The results show that the
18 variation in TEC corresponds well to the trend in solar parameters for most of the days observed during the study
19 period. Maximum TEC values were recorded at the equinoxes, while minimum values were observed at the
20 solstices. Other parameters will therefore need to be taken into account to explain this difference. In addition, the
21 variation in TEC as a function of EUV showed relatively small deviations from the variation due to F10.7 flux and
22 SN. This suggests that EUV may be more appropriate for modelling solar variation in TEC, particularly for long-
23 term trends. Finally, although the linear trend in solar variations in TEC was frequently observed, significant
24 saturation and amplification trends were also noted across the months and years analysed. This complexity in the
25 solar variation of TEC highlights the need for further studies to understand the effect of solar parameters on
26 TEC.health.

27
28 **Key words:-**

29 TEC, recurring geomagnetic days, Cycle solaire 24, Linear and quadratic model.
30
31
32
33

34 **Introduction:-**

35 Solar radiation is the main source of energy that causes the formation of the ionosphere. Research has established
36 that extreme ultraviolet (EUV) solar radiation and solar X-rays are the main sources of Earth's ionosphere formation
37 (from Adler et al., 1997). This solar radiation varies on different timescales, which has a significant impact on the
38 structure of the upper atmosphere, climate, and weather conditions, leading to remarkable changes in the Earth's
39 thermosphere and ionosphere (Hedin, 1984; Gorney, 1990). The critical parameter of the ionosphere, total electron
40 content (TEC), is attracting growing interest among researchers, particularly for studies of the equatorial ionosphere.
41 The Global Positioning System (GPS), widely used for space and terrestrial navigation, plays an essential role in
42 scientific research. Signals emitted by GPS satellites, propagating through the ionosphere located approximately 60-
43 1000 km above the Earth, are used to monitor the ionosphere on a global and regional scale (Rama Rao et al.,
44 2009; D'ujanga et al., 2012; Paznukhov et al., 2012) . The L1 (1575 MHz) and L2 (1228 MHz) frequencies
45 emitted by GPS satellites allow dual-frequency receivers to measure the ionospheric delay between them, generally
46 considered to follow the same path through the ionosphere. This approach has proven valuable for ionospheric
47 studies and opens up new research opportunities in this field. The amplitude of the TEC varies considerably in space
48 and time, depending on geomagnetic latitude, local time, season, solar activity, and geomagnetic activity (Soicher,
49 1988; Jakowski et al., 1999; B. Tsurutani et al., 2004) . By modelling TEC, it becomes possible to evaluate
50 ionospheric errors and correct them, particularly in the case of differential GPS.

51 Considerable research has been conducted worldwide to characterise the effects of solar activity on several
52 ionospheric parameters, such as electron density (Ne), plasma temperatures at different altitudes, total electron

53 content (TEC), maximum electron density (NmF2) and maximum height (hmF2) of the F2 layer, in terms of both
54 observations and theoretical models (Su et al., 1999; Kane, 2003; Lei et al., 2005; H. Liu et al., 2007) . In addition
55 to different regions of the globe, several researchers have studied the morphological characteristics of TEC, such as
56 diurnal, monthly, seasonal, latitudinal and solar activity variations, using various techniques, e.g. in
57 AfricaZoundial., , in South America ; on China (Zhao et al., 2007; G. Liu et al., 2013) , Huo et al.(2009) , and
58 Perevalova et al.(2010) ; on North America, Zakharenkova et al.(2013); on Japan, on Brazil , and manyothers.
59 Significantresults have been reported in the variability of TEC, whichis the parameterstudied in thiswork, in relation
60 to the solar cycle. Several authors have reported the dependence of TEC on solar activity at high, mid and low
61 latitudes (Balan et al., 1993; Afraimovich et al., 2008; Y. Chen et al., 2008) . Liu and Chen(2009)observed three
62 types of patterns (linearity, saturation and amplification) in TEC as a function of F10.7 radio flux. Therelationship
63 between TEC and solar indices (sunspot number (SN) and F10.7) or EUV solar flux is approximately linear (Balan
64 et al., 1993; Afraimovich et al., 2008) and quadratic (Y. Chen et al., 2008; L. Liu & Chen, 2009) . Recent work
65 shows that ionospheric parameters increase approximately linearly with solar indicators during low and medium
66 solar activity levels; however, they tend to saturate during high solar activity levels (Balan et al., 1994, 1994, 1996;
67 Gupta & Singh, 2000; Richards, 2001; Sethi et al., 2002; Lei et al., 2005) . The true manifestation of this
68 saturation effect is not yet fully understood.

69 Although TEC variations related to solar activity have been measured in different parts of the globe, little
70 work of this type has been undertaken around the equatorial region of the African continent, which has limited our
71 understanding of the equatorial ionosphere above Africa. Long-term records of TEC measurements are essential for
72 more accurately tracking the effects of solar activity on the equatorial ionosphere. During solar cycle 24,
73 characterised by different periods of solar activity and recurring geomagnetic events, it is essential to understand
74 how these solar variations affect the TEC at specific locations. The Koudougou station offers an ideal environment
75 for this study due to its geographical location and proximity to the magnetic equator. The ionospheric disturbances
76 observed at Koudougou are likely to be influenced by variations in solar activity and geomagnetic phenomena,
77 providing a unique opportunity to examine the impact of these factors on TEC. Using a detailed analysis approach
78 that includes statistical analysis techniques and accurate data on solar activity such as sunspots, solar flux F10.7 and
79 EUV flux, we aim to provide valuable insights into the relationship between solar activity and TEC at the
80 Koudougou station. The results of this study could contribute to a better understanding of the underlying physical
81 mechanisms and have significant implications for various fields such as satellite communications, navigation and
82 weather forecasting.

83 This article presents the TEC values measured by a SCINDA (Scintillation Network and Decision Aid)
84 dual-frequency GPS receiver located at Norbert Zongo University in Koudougou, Burkina Faso (Geo Lat 12°15'N;
85 Geo Long: -2°20'E) during solar cycle 24. The data used and the description of the methodology employed are
86 presented in Section 2. Section 3 concerns the analysis and interpretation of the results obtained.

87 **Data and methodology used**

88 **Data used**

89 The TEC data used in this work were obtained at the Koudougou GPS station (Geo lat 12°15'N; Geo long:
90 -2°20'E, dip: + 8.24). The GPS receiver at the Koudougou station was donated by the Ecole Nationale Supérieure
91 des Télécommunications de Bretagne (ENST-Bretagne, now Télécom-Bretagne) as part of the International
92 Heliophysical Year (IHY) project. This project mainly brings together three types of networks : (1) IGS
93 (International Geodesy System); (2) AMMA (Multidisciplinary Analysis of the African Monsoon), and (3)
94 SCINDA (Scintillation Network Decision Aid). The Koudougou station is one of the stations in the SCINDA GPS
95 network located at the equatorial latitude and dedicated to the study of ionospheric scintillations (OUATTARA et
96 al., 2011). Not listed in the global GPS station network, the Koudougou GPS station has been operating since
97 December 2008 and provides in situ data in RINEX format. The RINEX files used contain data recorded every 30
98 seconds. These RINEX files are then transformed to obtain the VTEC.

99 At the same time, precise measurements of solar activity, such as daily values for sunspot number (SN),
100 solar flux F10.7, and SOHO/SEM EUV flux (in wavelength ranges from 0.1 to 50 nm) were used to understand
101 variations in solar activity and its effects on TEC. The F10.7 index, which measures the radio flux at a wavelength
102 of 10.7 cm emitted by the Sun, and the sunspot number (SN) index, which indicates the number of sunspots present
103 on the Sun's surface and measures their intensity, are available on OMNIWeb at
104 <https://omniweb.gsfc.nasa.gov/form/dx1.html>. EUV (Extreme Ultraviolet) solar radiation, which is a form of
105 electromagnetic energy emitted by the outer layer of the solar atmosphere, can be downloaded from
106 http://lasp.colorado.edu/lisird/Whi_ref_spectra/.

107 Geomagnetic indices were also used in this work to select days of recurring geomagnetic activity. The
108 indices used are the disturbed storm time index (*Dst*), which indicates the hourly variation in the horizontal
109 component of the Earth's magnetic field (K. Patel et al., 2019) (http://isgi.unistra.fr/data_download.php) and the
110 interplanetary index *Kp*, which indicates the level of geomagnetic activity (Perira, 2004). The *Kp* values from the
111 OMNIweb database are available at <https://omniweb.gsfc.nasa.gov/form/dx1.html>.

112 Methodologies used

113 Statistical analysis and modelling

114 To analyse seasonal variations in TEC at the Koudougou station, we used TEC measurements for the spring
115 equinox (March, April, May), the summer solstice (June, July, August), the autumn equinox (September, October,
116 November) and the winter solstice (December, January, February) for the years 2010-2017. To indicate the
117 variability of solar activity, daily values for sunspot number (SN), solar flux F10.7 and EUV flux were used. In order
118 to see the variations in TEC during the different phases of a solar cycle, the annual average values of the SN solar
119 index from 2008 to 2018 (solar cycle 24 period) were used to divide the solar cycle into phases. The years 2008 and
120 2009, with average sunspot numbers (SN) of 2.8 and 3.1 (low solar activity) respectively, represent the minimum
121 phase of solar cycle 24, the years 2010 and 2011, with average SN numbers of 24.86 and 80.84 (moderate solar
122 activity) respectively, represent the ascending phase of cycle 24, the years 2012, 2013 and 2014, with average SN
123 numbers of 84.53; 94.02 and 113.34 (intense solar activity) respectively represent the maximum phase of solar cycle
124 24, and the years 2015, 2016, 2017 and 2018, with an average number of SNs of 69.82; 39.82; 21.74 (moderate solar
125 activity) and 6.97 (low solar activity) respectively represent the descending phase of solar cycle 24. However, the
126 TEC data available from the Koudougou station covers the period from 2010 to June 2017.

127 To assess the linear relationship between TEC and the SN, F10.7 and EUV solar indices, Pearson's
128 correlation coefficients, denoted *R*, were calculated for the annual, monthly and daily variation of TEC. A Pearson
129 correlation coefficient of 1 indicates a perfect positive linear correlation, a coefficient of -1 indicates a perfect
130 negative linear correlation, and 0 indicates no linear correlation. For all data used in this document, correlation
131 coefficient values (*R*) > 0.5 are considered highly significant.

132 Two regression models were also used to study the dependence of TEC on solar activity above Koudougou.
133 The first regression model is a linear approximation to describe the relationship between solar indices and TEC. A
134 linear model was proposed by Bassa et al. (1994), Bilitza (2000); Liu et al. (2003) to study the relationship between
135 TEC and solar activity. Its mathematical expression can be given by:

$$136 \quad TEC(S) = A_1 S + A_0 \quad (1)$$

137 The second regression model is the quadratic relationship between solar indices and TEC. A quadratic model was
138 proposed by Gupta et al. (2000); Sethi et al. (2002); Adewale et al. (2012); Kassa et al. (2017) to model the
variation in solar activity of TEC. Its mathematical expression can be given by:

$$139 \quad TEC(S) = A_2 S^2 + A_1 S + A_0 \quad (2)$$

139 where A_0 , A_1 , and A_2 are the unknown coefficients to be determined, and S represents solar activity, which could be
 140 evaluated by the number of sunspots (SN), the solar flux F10.7, or the EUV flux. The sign of A_2 indicates the
 141 possible non-linear trend, namely a tendency towards amplification for a positive A_2 , a tendency towards saturation
 142 for a negative A_2 , and a linear trend for an unknown A_2 .

143 Identification of recurring geomagnetic days

144 Recurrent geomagnetic activity refers to periodic variations in the Earth's magnetic field caused by the interaction
 145 between the fast solar wind and the Earth's magnetosphere or by co-rotating interaction regions (CIRs) (B. T.
 146 Tsurutani et al., 2006). Legrand and Simon (1989) have classified geomagnetic activity into four classes: (1) quiet
 147 activity characterised by $Aa < 20 \text{ nT}$, (2) shock activity caused by SSCs and characterised by $Aa \geq 40 \text{ nT}$, (3)
 148 recurrent activity characterised by $Aa \geq 40 \text{ nT}$ without SSCs and repeating over two or more Bartels rotations, and
 149 (4) fluctuating activity, which is activity not covered by the other three classes. This classification was later
 150 improved by Ouattara and Amory Mazaudier (2009), who introduced a colour-coding system to graphically
 151 represent the different classes on a pixel diagram. More recently, Zerbo et al. (2012) have also made improvements
 152 to this classification. This present work focuses on the class of recurrent geomagnetic activity days. This work
 153 considers geomagnetically disturbed days that meet the following criteria to be recurring days: $Kp \geq 27$ and $Dst \leq$
 154 -30 nT , with a periodicity of 27 days. In order to eliminate the influence of other geomagnetic events, all recurring
 155 days preceded by an SSC (Sudden Storm Commencement) or an SI (Sudden Impulse) occurring in the previous
 156 three days were excluded. Taking into account the conditions set, the occurrence of recurring geomagnetic days is
 157 established in Table 1. It should be noted that these days correspond to the days when TEC data are available at the
 158 Koudougou station.

159 Table 1: Occurrence of recurring geomagnetic days during cycle 24

Year	2008	2009	2010	2011	2012	2013	2014	2015	2016	2017	2018
Recurring days	0	1	9	31	37	31	69	133	100	50	0

160 Results and discussions

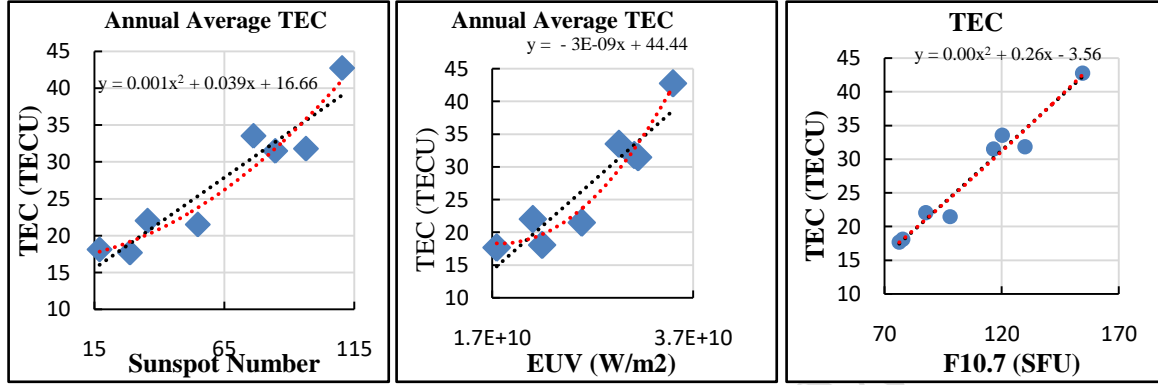
161 Correlation between the average annual TEC and the SN, F10.7, and EUV solar indices

162 In order to verify the dependence of TEC on solar activity during recurring geomagnetic periods, we obtained the
 163 statistical correlation between the average annual TEC and the number of sunspots (SN), the solar flux F10.7 and the
 164 EUV flux at the Koudougou station. Figure 2 shows the scatter plots and correlation analysis between the annual
 165 average TEC values and the number of sunspots (SN), solar flux F10.7 and EUV flux during the period 2010-2017.
 166 Panels a, b and c of Figure 2 show the scatter plots of the annual TEC values as a function of SN, F10.7 and EUV,
 167 respectively. To model the average annual variations in Total Electron Content (TEC) as a function of solar activity,
 168 linear and quadratic adjustments were applied. Pearson's correlation coefficients (R) between the average annual
 169 TEC and the index (SN), solar flux F10.7 and EUV flux during recurring geomagnetic periods in Koudougou are
 170 calculated and presented in **Table 2**.

171 The graphs in Figure 2 clearly show that all solar indices are strongly correlated with the average annual
 172 TEC at the Koudougou station. The average annual variation in TEC as a function of the three solar indices
 173 considered showed a positive correlation. The correlation coefficients of SN, F10.7 and EUV flux with TEC are
 174 0.94, 0.98 and 0.93, respectively. This shows that TEC follows an almost one-to-one correlation with these solar
 175 indices. This strong correlation between TEC and solar activity indicates a strong positive linear relationship
 176 between these two series. The high degree of correlation obtained for these solar activity indices suggests that the
 177 production and ionisation of the ionosphere and its dynamics are entirely controlled by the level of solar radiation
 178 received by the ionosphere and that the ionosphere varies closely with it. Consequently, the variability of the
 179 ionosphere will also follow the cyclical variability of solar activity.

180 **Table 2:** Correlation coefficients between TEC and solar parameters (SN, F10.7 and EUV) on a time resolution of
 181 one year

Solar indices	SN	F10.7	EUV
Annual TEC	0.94	0.98	0.93



182 **Figure 2:** Scatter plots of annual mean TEC values and solar parameters (SN, F10.7 and EUV) from 2010 to 2017
 183 during recurrent geomagnetic activity.

184 From the general expression of the quadratic model given by equation (2), we can deduce the degree of linear and
 185 non-linear variation in the TEC observation as a function of solar parameters. The sign of the coefficient A_2 indicates
 186 possible non-linear variations (trends) in the TEC due to variations in the corresponding solar indices SN, F10.7 or
 187 EUV. The graphs in Figure 2 show linear and non-linear trends. Panel c of Figure 2 shows a linear variation of the
 188 TEC as a function of the solar index F10.7. However, panels a and b indicate a non-linear variation of the TEC as a
 189 function of SN and EUV. The quadratic equations for these different variations are:

$$TEC = 0,0016(SN)^2 + 0,0399(SN) + 16,664 \quad (3)$$

$$TEC = 8.10^{-20}(EUV)^2 - 3.10^{-9}(EUV) + 44,443 \quad (4)$$

$$TEC = 0,00(F10.7)^2 + 0,26(F10.7) - 3,56 \quad (5)$$

190 The coefficient A_2 of equation (5) indicates the existence of a linear relationship ($A_2 = 0$) between the average
 191 annual variation in TEC and the solar flux F10.7. This assumes that the average annual TEC varies proportionally to
 192 the solar index F10.7, with a constant slope. However, equations (3) and (4) illustrate the existence of an
 193 amplification ($A_2 > 0$) between the average annual TEC and the number of sunspots and the EUV flux, respectively.
 194 This allows us to model a quadratic relationship between the TEC and solar activity. Furthermore, no hysteresis
 195 effect was observed in this annual variation. This absence of hysteresis can be explained by the large time gap
 196 between two consecutive values in the time series (up to one year). Therefore, let us aim for an analysis with a time
 197 interval.

198 **Monthly variation in TEC with solar indices SN, F10.7, and EUV**

199 To study the seasonal variation of GPS-TEC for different years (2010–2016), each year was classified into four
 200 seasons, namely the spring equinox (March, April, May), the autumn equinox (September, October and November),
 201 the summer solstice (June, July and August) and the winter solstice (December of the previous year and January,
 202 February of the current year). To do this, graphs showing monthly TEC variations based on solar indices for each
 203 year will be considered. The curves in **Figure 3** illustrate these variations above Koudougou. These curves are
 204 produced taking into account all recurring geomagnetic days. The left column shows the variation in TEC as a

205 function of SN, the middle column describes the average monthly TEC as a function of F10.7, and the right column
206 shows the variation in TEC as a function of EUV from 2010 to 2016. In all panels, the red histograms indicate the
207 average monthly TEC, and the black curves show the variations in solar indices. The seasonal variation is studied
208 for each year from 2010 to 2017 to determine in detail the effect of the phases of the solar cycle and the
209 characteristics of the different levels of solar activity. Consequently, the panels are classified by year in ascending
210 order from top to bottom.

211 The month-to-month variation in TEC shown in Figure 3 explains the variation in TEC in response to solar
212 activity by superimposing the values of the solar parameters on the same graph. The solar parameters indicate that
213 2010 was a relatively quiet year, recording moderate values. The curves show that the solar parameters SN, F10.7
214 and EUV have similar monthly variations in 2012 and different variations in other years. In addition, identical
215 variations in the SN and F10.7 parameters are observed in 2011 and 2016, with significant increases in SN in 2016.
216 For F10.7 and EUV, identical variations are observed in 2013 and 2015.

UNDER PEER REVIEW IN IJARI



Figure 3: Monthly variations in TEC as a function of the solar parameters SN, F10.7 and EUV from 2010 to 2017

217

218

219

Such differences in the variation of solar indices have been reported by **Chakrabarty et al.(2012)** , who observed divergences in these parameters above the region of the equatorial anomaly ridge. With regard to the variation of

220 these parameters with TEC, they reported a direct solar influence on TEC. In our results (**Figure 3**), we observe that
221 while the TEC trend tends to follow that of the solar parameters, the rate of increase of these solar parameters is
222 much higher than that of the monthly mean TEC. Such results were reported by **D'ujanga et al.**(2016) in the
223 Kampala region of Uganda. In general, the mean TEC values are relatively high in March, April, May, October, and
224 November and low in January, June, July, August, and December. However, solar parameters show random
225 variations during the study period. In particular, the months of June, July, and August 2012 saw drastic increases in
226 solar parameters, which did not correspond to the increase in TEC during these months. At the same time, the
227 maximum F10.7 solar flux in 2013 was observed in December, with a corresponding increase in EUV, while TEC
228 values showed higher values in March and October 2013. In fact, the equinoctial months of March, April, and May
229 (vernal) and September, October, and November (autumnal) showed much higher TEC values than the solstice
230 months during the observation period. This is consistent with most research conducted in equatorial regions (**Gupta
231 & Singh, 2000; Chauhan et al., 2011; Olwendo et al., 2013**). Upon closer examination, however, it can be
232 observed that the TEC for the solstice months of July and August 2012 is higher than for the same months in 2010
233 and 2011, when the SN, F10.7 solar flux, and EUV flux were relatively weaker. This shows the interdependence of
234 seasonal and solar parameters, while noting that the TEC responds more to seasonal variations than to variations in
235 solar parameters at the Koudougou station.

236 It was also observed that the autumn months (September, October, and November) had slightly higher TEC
237 values than the spring equinoxes (March, April, and May) in 2010, 2012, and 2013, years that saw a sharp increase
238 in solar activity (Figure 3). In contrast, the years 2015 and 2016 (descending phase of solar cycle 24) showed a
239 reverse equinoctial asymmetry, with the TEC of the spring equinox being slightly higher than that of the autumn
240 equinox. However, the year of the solar maximum (2014) shows almost equal TEC values at both equinoxes.
241 Indeed, during the solar maximum, it is known that during the equinoxes, the Sun crosses the equator and, as a
242 result, the period of maximum sunshine is the same at the spring and autumn equinoxes at equatorial stations. The
243 equinoctial asymmetry observed during the ascending phase (2010, 2012, and 2013) differs from that observed by
244 various researchers who reported the opposite when studying different parameters. For example, **Sripathi et
245 al.**(2011) observed higher TEC values during the spring equinox than during the autumn equinox, and a higher
246 occurrence of scintillation was observed during the spring equinox than during the autumn equinox by **Rama Rao et
247 al.**(2006). In all these cases, equinoctial asymmetry was attributed to differences in meridional winds, leading to
248 changes in neutral composition during the equinoxes. The difference observed in equinoctial asymmetry during the
249 descending phase (2015-2016) could be due to the direct effects of solar activity, since during these years, spring
250 recorded higher solar parameter values (SN, F10.7, and EUV) than autumn, leading to higher ambient ionisation
251 during this period. The difference in equinoctial asymmetry during the different phases of cycle 24 could be due to
252 the geomagnetic activity class chosen. Indeed, the occurrence of recurring days shows a higher number of days in
253 2015 and 2016 than in other years.

254 Compared to other seasons, the summer TEC is lowest for the years 2013, 2014, 2015, and 2016. However,
255 for the years 2010, 2011, and 2012, the lowest TEC is observed during the winter months. Furthermore, the increase
256 in TEC in winter compared to summer for the years mentioned at low latitudes above the Koudougou station shows
257 a "winter anomaly". The most motivating aspect of TEC observations at low latitudes, which has been studied by a
258 number of researchers, is the presence of a winter anomaly in the ridge region of the; while other researchers have
259 also studied the disappearance of the "winter anomaly" (Balan et al., 1993; Bhuyan & Hazarika, 2013; Galav et al.,
260 2010; Lin et al., 2007). The "winter anomaly" is defined by the fact that winter electron density remains higher than
261 summer electron density (Rishbeth and Garriot). The winter anomaly is caused by the increase in the (O/N₂) ratio in
262 the thermosphere between the southern hemisphere and the northern hemisphere, as reported by a number of
263 authors. Thus, the appearance of the winter anomaly in the peak strength of the EIA has been attributed to a
264 difference in energy input between the southern hemisphere and the northern hemisphere (Torr & Torr, 1973); to the
265 change of season by a neutral gas composition (Mukherjee et al., 2010; Aggarwal et al., 2012). Research conducted

266 by Kumar et al.(2014) added that this could be due to a combined effect of the geometry of the magnetic field and
267 the zenith angle of the sun.

268 The differences observed in the monthly TEC values may also be due to geomagnetic storms, which can
269 sometimes affect the ionosphere and alter it in complex and unpredictable ways, especially since the class chosen is
270 a class of disturbed geomagnetic activity. A review of the (Dst) and (Kp) indices for the years 2010-2016 indicates
271 that 2010 did not experience any severe geomagnetic storms, except for a few moderate storms (Dst> -100) over a
272 few days, while 2011, 2012 and 2013 experienced a few intense geomagnetic storms (Dst< -100) in September and
273 October 2011, March, October and November 2012, and March and June 2013. However, many more moderate and
274 intense geomagnetic storms were observed in 2015 and 2016. It has been reported that magnetic storms have effects
275 on the TEC in the equatorial region, with some showing an increase in TEC and others a decrease in TEC,
276 accompanied by ionospheric scintillations (Akala, Rabiou, et al., 2013; D'ujanga et al., 2013). These effects on
277 TEC can cause intense phase and amplitude scintillations in satellite signals, thereby negatively impacting satellite
278 communication and navigation systems. To quantify the impact of solar activity on monthly TEC variations at the
279 Koudougou station, linear and quadratic adjustments between monthly TEC variations and the SN, F10.7, and EUV
280 solar indices will be established.

281 **Correlation of the monthly average TEC with the SN, F10.7, and EUV solar indices**

282 To statistically analyse the variation in the average monthly TEC based on the SN, F10.7, and EUV solar
283 indices, a series of scatter plots was constructed for each year from 2010 to 2016, as shown in Figure 4, in order to
284 determine which solar index correlates well with the TEC in Koudougou. The left-hand columns illustrate the
285 relationship between TEC and the SN index, while the middle column shows the relationship between TEC and the
286 F10.7 index, and, finally, the right-hand column shows the relationship between TEC and the EUV index. To
287 determine the best possible relationship between monthly TEC values and the SN, F10.7, and EUV solar indices,
288 linear (represented by black dotted lines) and quadratic (represented by red dotted lines) adjustments were applied to
289 the data. In order to analyse the correlation, Pearson's correlation coefficients between the monthly average TEC and
290 the SN, F10.7, and EUV solar indices for each year were calculated. These coefficients are presented and ranked in
291 Table 3.

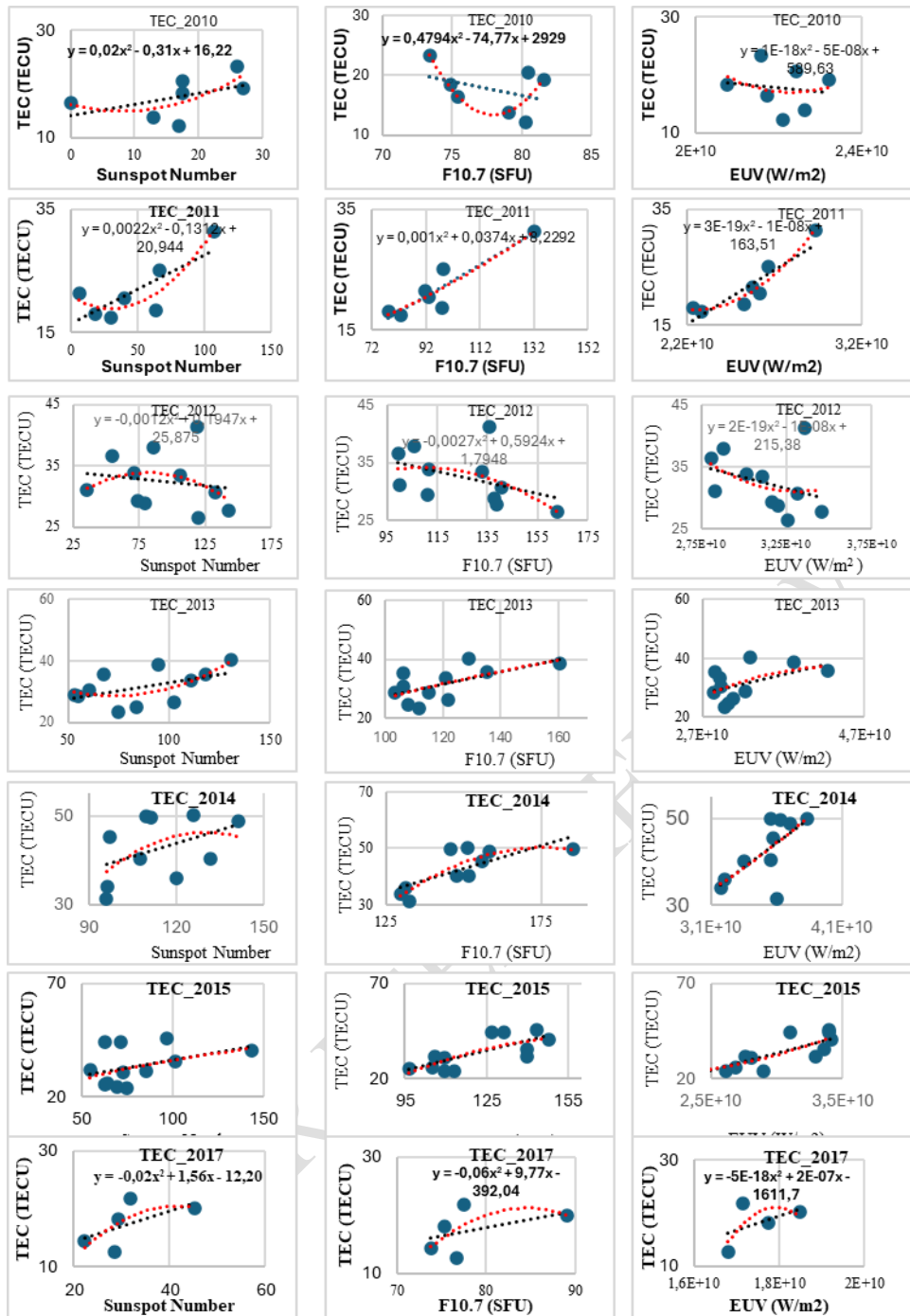
292 The scatter plots from 2010 to 2016 (Figure 4) show that there is a significant difference in the relationship
293 between the average monthly TEC and the solar indices for the different years considered. The correlation between
294 the two is remarkable (high) during years of fairly moderate solar activity (2011 and 2016). Negative correlation
295 coefficients between TEC and the F10.7 and EUV solar indices are observed in 2010 and 2012, and between TEC
296 and SN in 2012. Significant correlation coefficients ($R > 0,5$) between TEC and SN are observed in 2011, 2013,
297 and 2016. $R > 0,5$ is observed in the relationship with F10.7 in 2011, 2013, 2014, 2015, and 2016, and with EUV in
298 2011, 2014, 2015, and 2016. The positive and negative correlation coefficients with the various solar indices have
299 also been reported by other researchers (Kumar & Singh, 2009; N. C. Patel et al., 2017). However, Patel et al.
300 (2017) found positive correlation coefficients between TEC and F10.7 and between TEC and EUV in 2010 and 2012
301 and negative correlation coefficients between TEC and all three solar indices in 2013, which is contrary to our
302 results. Furthermore, work by Kumar and Singh(2009) during the period 2007-2009 showed weaker correlation
303 coefficients between TEC and SN. On the other hand, research conducted by Galav et al.(2010) for the period 2005
304 to 2009, and Opio et al.(2015) in 2011 showed higher coefficients ($R>0.70$) between TEC and F10.7. At the
305 Koudougou station, with a monthly time resolution, the correlation coefficients are relatively higher with the F10.7
306 index than with the SN and EUV indices. Also, a weaker correlation is observed between TEC and SN, with the
307 exception of 2011 and 2016. This indicates that the monthly variation in TEC is weakly related to sunspot activity.
308 The weak correlations observed in some years suggest that the production and ionisation of the ionosphere and its
309 dynamics are not entirely controlled by the level of solar radiation received by the ionosphere.

310 The scatter plots in Figure 4 show the ability of the quadratic model to represent the non-linear variation of
311 the TEC as a function of SN, EUV flux and F10.7. In general, the model output showed varying degrees of

312 agreement with the values measured during the different months. From the general expression of the quadratic
 313 model given by equation (2), we can deduce the degree of linear and non-linear variation of the TEC as a function of
 314 solar parameters. Therefore, Figure 4 indicates the existence of linearity ($A_2 = 0$) between TEC and SN in 2015 and
 315 2016, TEC and F10.7 in 2011 and 2013, and between TEC and EUV in 2014, 2015, and 2016. The existence of
 316 amplification ($A_2 > 0$) between TEC and SN is observed in 2010, 2011, and 2013, and saturation ($A_2 < 0$) in 2012 and
 317 2014. Saturation and amplification trends between TEC and F10.7 are observed in 2012, 2014, and 2015, and 2010,
 318 2016, respectively. With the EUV index, saturation trends are observed in **2017** and amplification trends in 2010,
 319 2011, and 2012. The linear fit between TEC and solar indices shows an increasing trend in all years except 2012 and
 320 2010 with the F10.7 index and the EUV index. The analysis of quality statistics illustrated by the graphical
 321 equations presented in each panel of Figure 4 shows that the non-linearity coefficient is relatively low (close to 10^{-3})
 322 for all years and for all solar indices considered. This shows that quadratic and linear adjustments give almost
 323 similar results for all months and years considered. This result shows that, for application purposes, linear or
 324 quadratic regressions may be a good choice and that higher-order regressions do not significantly improve the fit.

325 Table 3: Correlation coefficients between TEC and solar parameters (SN, F10.7, and EUV)

Year Solar Indices	2010	2011	2012	2013	2014	2015	2016	2017
SN	0.49	0.77	-0.16	0.52	0.44	0.40	0.72	0.59
F10.7	-0.38	0.91	-0.43	0.62	0.74	0.74	0.66	0.47
EUV	-0.14	0.90	-0.33	0.50	0.67	0.79	0.66	0.49



326

327 **Figure 4:** Scatter plots of monthly mean TEC values and solar parameters (SN, F10.7, and EUV) from 2010 to 2017
 328 during recurrent geomagnetic activity

329 **Variation in average daily TEC with solar indices SN, F10.7, and EUV**

330 The daily variations in TEC as a function of sunspot number, solar flux F10.7, and EUV flux during the
 331 period 2010-2017 are shown in the top, middle, and bottom panels of **Figure 5**, respectively. The blue curves
 332 indicate the daily variations in TEC, and the red curves indicate those in solar indices. Each graph representing the
 333 daily variation for a given year is constructed considering all recurring geomagnetic days of the year. The study of

334 daily variation is intended to verify the behaviour of TEC as a function of solar activity on a reduced time scale for
335 the period 2010 to 2017 in order to identify the effects of short-term solar activity on TEC.

336 As shown in the panels in Figure 5, the curves of the daily variations in solar indices did not show good
337 agreement with the daily TEC values for all the years considered. Contrary results were reported by **Kassa et**
338 **al.**(2017) during the final phase of solar cycle 23 and the ascending phase of solar cycle 24, who found good
339 agreement between the TEC curves and those of the SN and F10.7 solar indices on a daily scale. Nevertheless, it
340 was found that the TEC curve and the solar indices curve appeared to be much more in phase in 2011, 2015, and
341 2016 than in other years. In contrast, in 2012, a high TEC value corresponded to a low SN, F10.7, and EUV value,
342 except on the 182nd day of the year, when the trough of the TEC curve and that of the solar indices overlap. In
343 2010, 2013, and 2014, the two curves evolve in phase, but with the peaks of the solar indices slightly offset from
344 those of the TEC. The same phenomenon is observed during the descending phase of cycle 24, but with a less
345 pronounced effect. In all the graphs presented (2010-2016), the TEC curve is more in phase with the F10.7 solar flux
346 and the EUV flux than with the number of sunspots, and much more in line with the EUV flux. According to **Prasad**
347 **et al.**(2012), the F10.7 index comes mainly from the high-temperature transition region of the solar atmosphere, but
348 the solar EUV flux comes from the irregular layer above the photosphere ("Chromosphere") and, to a lesser extent,
349 from the transition region and the corona. During periods of high solar activity, the F10.7 flux undergoes greater
350 fluctuations, and the EUV emissions from the most excited atoms in the solar atmosphere correlate with TEC.

351 A very important notable feature is the daily uncertainty in TEC variation, which is of great concern for
352 forecasting as well as for navigation systems. This uncertainty in the daily and seasonal variation of TEC (**Kane,**
353 **1980; Rama Rao et al., 2006; Rao et al., 2013**) can be attributed to: 1) changes in the activity of the Sun itself and
354 related changes in the intensity of incoming radiation; 2) the zenith angle (γ) at which they reach the Earth's upper
355 atmosphere, in addition to changes in the Earth's magnetic field; 3) the strength of the equatorial electrojet (EEJ),
356 added to the effects due to EIA dynamics; and 4) neutral meridional winds. The diurnal variation in TEC may also
357 be due to the movement of ionised particles through geomagnetic fields by tidal winds (**Tariku, 2015**). Recently,
358 **Jonah et al.**(2015) studied the variation in TEC during phases of high and low solar activity over the South
359 American sector. They indicated that a diurnal uncertainty in the variation in TEC contains a component induced by
360 planetary waves enhanced by tides as they propagate upwards. Strong vertical coupling through increasingly
361 propagating waves can also give rise to a daily oscillation in TEC. Their study also shows that, apart from the effect
362 of solar radiation, variations in the meridional or zonal wind also play an important role in TEC variations.

363

364

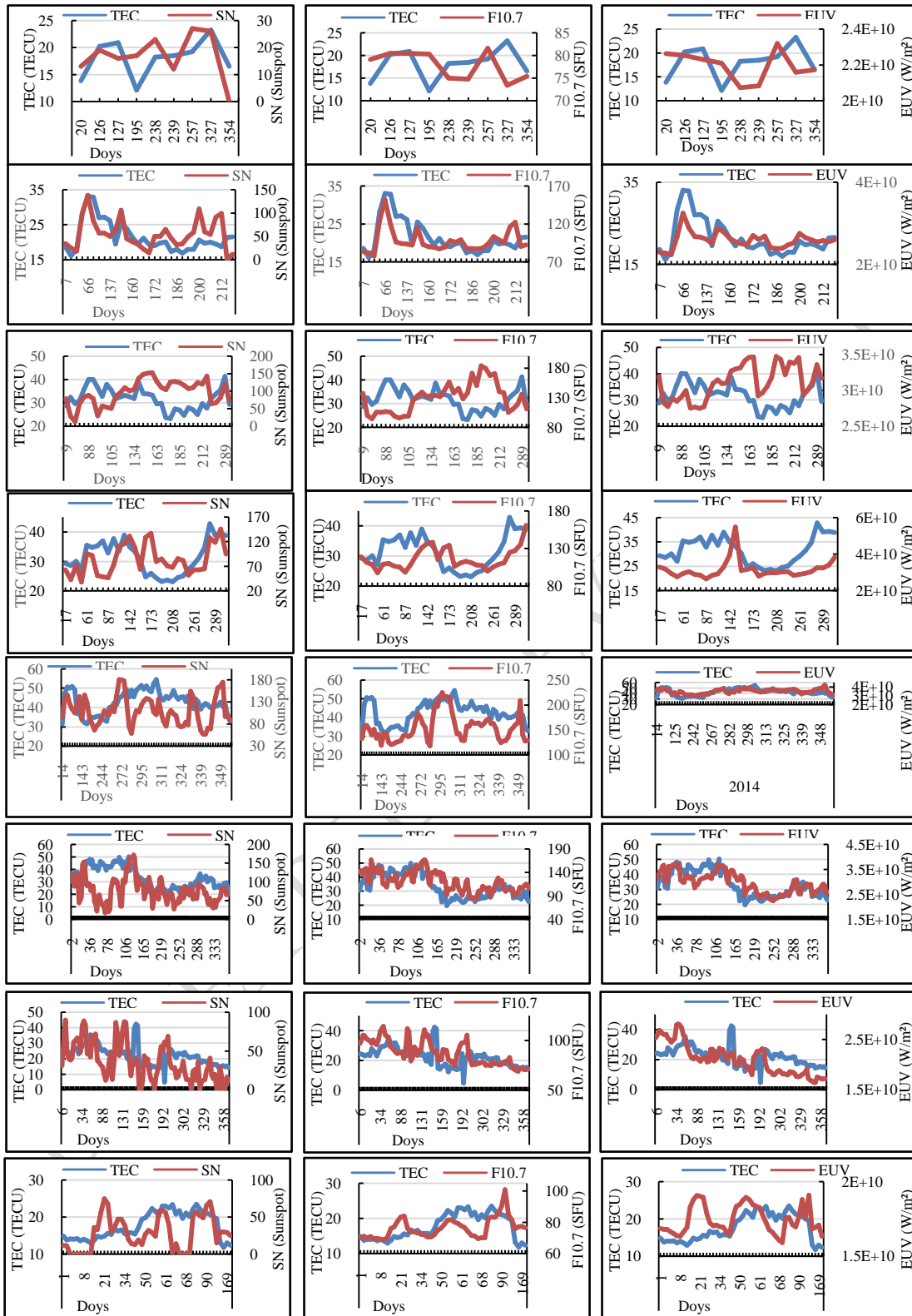
365

366

367

368

369



370 Figure 5: Daily variation in TEC as a function of solar parameters SN, F10.7, and EUV from 2010 to 2017

371

Correlation of average daily TEC with solar indices SN, F10.7, and EUV

The correlation coefficients between solar indices (SN, F10.7, and EUV) and the average daily TEC in Koudougou for all years during the period 2010–2016 were determined in order to find the dependence of TEC on solar activity at a fairly short time interval. These coefficients are presented and classified in Table 4. Only geomagnetically disturbed days with ($K_p > 27$) and with a periodicity of 27 days were selected to highlight the effect of this class of geomagnetic activity on the TEC from one day to the next. Scatter plots between SN and TEC, F10.7 and TEC, and EUV and TEC were also constructed. Since the scatter plots were constructed for series with a time resolution of one day, the daily average series of solar activity parameters were used. Figure 6 shows these scatter plots for each year from 2010 to 2016. The left column illustrates the relationship between TEC and the SN index, while the middle column shows the relationship between TEC and the F10.7 index, and finally, the right column shows the relationship between TEC and the EUV index. Linear (represented by black dotted lines) and quadratic (represented by red dotted lines) adjustments were also applied to observe trends in the relationship between these two parameters.

Table 4 shows that the correlation coefficients between TEC and solar indices are weaker daily than on a monthly and annual basis between 2010 and 2016 at the Koudougou station. This means that the impact of solar activity on TEC variation is reduced when the time interval considered is also reduced. This implies that there may be other parameters besides solar proxies that can affect TEC variation daily. A detailed analysis of Table 4 shows a negative correlation coefficient between the average daily TEC and the three solar indices in 2012 and between TEC and F10.7 and EUV in 2010. A significant positive correlation between average daily TEC and SN is observed only in 2011 ($R = 0.52$). However, between TEC and F10.7, it is significant and positive in 2011 ($R = 0.67$), 2014 ($R = 0.59$), and 2015 ($R = 0.68$), and negative in 2012 ($R = -0.55$). Only a significant positive correlation is observed between TEC and EUV in 2011 ($R = 0.79$), 2014 ($R = 0.59$), 2015 ($R = 0.76$), and 2016 ($R = 0.51$). The panels in Figure 6 show that the trend between TEC and solar indices is increasing for all years except 2012 and 2010 with the F10.7 index and the EUV index. The correlation analysis results presented show relatively high and relatively low correlations between the TEC series and solar parameters. Therefore, the linear regression method (high correlation) and the quadratic regression method (low correlation) can be used to reconstruct TEC variations using solar parameters as inputs. This will prove the physical relationships between ionospheric and solar parameters. However, to obtain the best possible prediction quality, we can use parameters as inputs that could be related to each other (both by physical and statistical processes). Similar, but not exactly the same, approaches were adopted by **Chen et al.**(2015) and **Li et al.**(2019) to model TEC variations over large areas as a function of solar activity (F10.7 index) and geomagnetic activity (A_p index). Similarly, in the article published by **Morozova et al.**(2020), this approach was adopted to achieve the best possible prediction quality between TEC series and space weather parameters in the Iberian Peninsula.

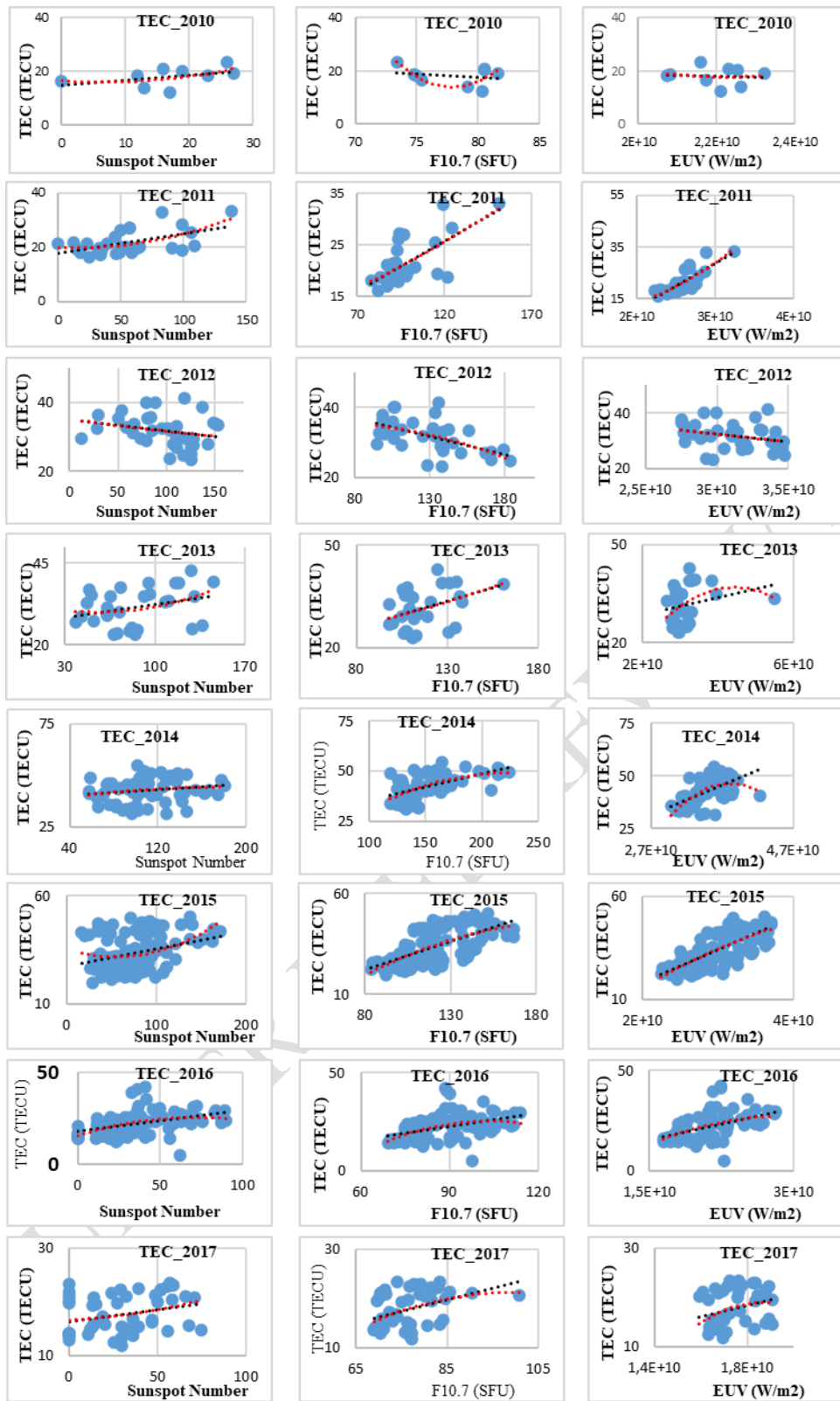
Table 4: Correlation coefficients between TEC and solar parameters (SN, F10.7, and EUV) at a temporal resolution of one day.

Year Solar indices	2010	2011	2012	2013	2014	2015	2016	2017
SN	0.44	0.52	-0.26	0.31	0.17	0.31	0.44	0.28
F10.7	-0.26	0.67	-0.55	0.39	0.59	0.68	0.44	0.42
EUV	-0.10	0.79	-0.29	0.23	0.59	0.76	0.51	0.29

407

408 In general, the model output showed varying degrees of agreement with the values measured during the different
409 months. In almost all cases, the daily variation in TEC for each year showed positive correlations with solar indices.
410 Linear correlations between solar indices and TEC were also observed. Our observations are consistent with the
411 report by Liu and Chen(2009), who showed a very close correlation between maximum TEC and the number of
412 sunspots in March, May, August, September, and December, while a weak correlation was observed in February and
413 July of the 2003 high solar activity period in Hong Kong. From a detailed analysis of the graphs in Figure 6, we can
414 deduce the degree of linear and non-linear variation in TEC as a function of solar parameters. Figure 6, therefore,
415 indicates the existence of linearity ($A_2 = 0$) between TEC and SN in 2012, TEC and F10.7 in 2011 and 2013, and
416 TEC and EUV in 2011 and 2012. The existence of amplification ($A_2 > 0$) between TEC and SN is observed in almost
417 all years except 2012, 2014, and 2016, where saturation ($A_2 < 0$) is observed. The saturation trends between TEC and

UNDER PEER REVIEW IN IJAE



418

419 **Figure 6:** Scatter plots of average TEC values and solar parameters (SN, F10.7 and EUV) from 2010 to 2017 during
 420 recurrent geomagnetic activity with a time resolution of one day.

421 F10.7 are observed in 2012, 2014, 2015, 2016 and 2017 and amplification in 2010. With the EUV index,
422 amplification trends are observed in 2010 and saturation in 2013 and 2017. The linear fit between TEC and solar
423 indices shows an increasing trend in all years except 2012 and 2010 with the F10.7 index and the EUV index.
424 Relatively small deviations were observed in the modelling of TEC as a function of EUV compared to the variation
425 due to F10.7 flux and SN. This may indicate that EUV may be more appropriate for modelling solar variation in
426 TEC. Analysis of the quality statistics shows that the non-linearity coefficient is relatively small (10^{-3}) for all years
427 and for all solar indices considered. This shows that quadratic and linear adjustments give almost similar results for
428 all years considered. This result shows that, for application purposes, linear or quadratic regressions may be a good
429 choice and that higher-order regressions do not significantly improve the fit.

430 Consequently, the effects of solar activity on electron density in the ionosphere show an interesting altitude
431 dependence (Su et al., 1999) and the behaviour of TEC and NmF2 may differ in some respects. Linear and
432 saturation effects are observed in the dependence of solar activity on diurnal NmF2 or foF2 (Lei et al., 2005; L. Liu
433 et al., 2006; Zhang & Holt, 2007). The amplification effect can sometimes be detected in nocturnal NmF2 (L. Liu
434 et al., 2004). Linearity, saturation and amplification patterns can all be found at low latitudes at different local times
435 (L. Liu & Chen, 2009); this explains why the dependence of solar activity on TEC at this altitude varies according
436 to local time, season and location. Complex patterns are also observed, as shown in the results in Figure 6. The most
437 fascinating feature is the amplification of TEC. Previous studies (Balan et al., 1994; Afraimovich et al., 2008;
438 Chakraborty & Hajra, 2008) have mainly focused on linearity and saturation. This amplification effect in the TEC
439 is a new feature.

440 Ion production in the ionosphere is proportional to EUV flux, which can be related to ambient electron
441 density. However, ionisation by direct solar flux is not the only cause of changes in electron density. Changes can
442 also occur due to alterations in neutral density, temperature, and composition, ionospheric chemistry, neutral winds
443 (L. Liu et al., 2004), and electric fields, all of which vary with solar EUV and whose relationship to electron
444 density may not be linear (Kane, 2003). The complex patterns in the effects of solar activity on the TEC can be
445 explained qualitatively in the discussion by Chen et al. (2009) and Liu et al. (2007), if we realise that the neutral
446 compositions in the upper atmosphere, ionospheric scale heights, and dynamic processes also vary with solar
447 activity (Kutiev et al., 2006; L. Liu et al., 2004). We can understand the TEC amplification effect qualitatively as
448 follows. As a first approximation, the electron density profile obeys a Chapman-type function; the TEC is therefore
449 related to the scale height H and the maximum electron density NmF2.

450 Conclusion

451 This study showed that annual variations in Total Electron Content (TEC) at the Koudougou station are
452 closely linked to solar parameters such as sunspot number (SN), solar flux F10.7 and extreme ultraviolet flux
453 (EUV). The results revealed that TEC follows an extraordinary synchronisation with solar activity during periods of
454 recurrent geomagnetic activity. Variations in TEC showed a strong correlation with solar indices, indicating a
455 positive linear relationship between these two series. The graphs showed that TEC primarily tracks variations in
456 EUV flux rather than those in solar flux F10.7 and sunspot number. This is consistent with previous research that
457 established extreme ultraviolet (EUV) solar radiation as the primary source of Earth's ionosphere formation.
458 Analysis of monthly and daily data showed that the impact of solar activity on TEC variation decreases when the
459 time interval considered is shorter. This suggests that other parameters, in addition to solar indices, could influence
460 daily TEC variation. Using linear and quadratic regression models, it is possible to reconstruct TEC variations using
461 solar parameters as inputs. However, to obtain better prediction quality, it may be beneficial to include other
462 parameters that are interrelated, both physically and statistically.

463 Furthermore, it has been found that during the solstice months of the year, TEC shows a downward trend in
464 line with the decrease in solar parameters. It has also been demonstrated that the solstice is a relatively stable season
465 with insignificant average day-to-day TEC variation, indicating a reduced influence of external factors. Also, the
466 linear trend of TEC as a function of solar activity indices, accompanied by some non-linear solar variations

467 (saturation and amplification) of TEC, has been observed. This mixed trend of solar variation in TEC implies the
468 need for further study of the effect of solar parameters on TEC. However, based on a long-term dataset, we have
469 concluded that solar variations in TEC are dominated by a linear model. From a general perspective, estimating TEC
470 using the quadratic model is valid, but on certain specific days, external factors highlight the occurrence of
471 significant errors. Therefore, further research may be necessary to delve deeper into this complex relationship and
472 explore other factors that may influence TEC variability.

473 **Data availability**

474 The total electron content (TEC) data used to support the results of this study are included in the
475 supplementary file(s). The F10.7 solar flux index and the Kp index are available on the OMNIWeb website
476 (<https://omniweb.gsfc.nasa.gov/form/dx1.html>). The geomagnetic index (Dst) data used are available on the ISGI
477 website (http://isgi.unistra.fr/data_download.php). The sunspot number data used in this work are available on the
478 SILSO website (<https://www.sidc.be/silso/datafiles>).

479 **Conflicts of interest**

480

481 The authors have declared no conflicts of interest.

482 **References**

483

- 484 Adewale, A. O., Oyeyemi, E. O., & Olwendo, J. (2012). Solar activity dependence of total electron content derived
485 from GPS observations over Mbarara. *Advances in Space Research*, 50(4), 415-
- 486 Afraimovich, E. L., Astafyeva, E. I., Oinats, A. V., Yasukevich, Y. V., & Zhivetiev, I. V. (2008). Global electron
487 content: A new conception to track solar activity. *Annales Geophysicae*, 26(2), 335-344.
- 488 Aggarwal, M., Joshi, H. P., Iyer, K. N., Kwak, Y.-S., Lee, J. J., Chandra, H., & Cho, K. S. (2012). Day-to-day
489 variability of equatorial anomaly in GPS-TEC during low solar activity period. *Advances in Space Research*, 49(12),
490 1709-1720.
- 491 Akala, A. O., Rabiou, A. B., Somoye, E. O., Oyeyemi, E. O., & Adeloye, A. B. (2013). The Response of African
492 equatorial GPS-TEC to intense geomagnetic storms during the ascending phase of solar cycle 24. *Journal of*
493 *Atmospheric and Solar-Terrestrial Physics*, 98, 50-62.
- 494 Akala, A. O., Seemala, G. K., Doherty, P. H., Valladares, C. E., Carrano, C. S., Espinoza, J., & Oluyo, S. (2013).
495 Comparison of equatorial GPS-TEC observations over an African station and an American station during the
496 minimum and ascending phases of solar cycle 24. *Annales Geophysicae*, 31(11), 2085-2096.
- 497 Balan, N., Bailey, G. J., & Jayachandran, B. (1993). Ionospheric evidence for a nonlinear relationship between the
498 solar EUV and 10.7 cm fluxes during an intense solar cycle. *Planetary and Space Science*, 41(2), 141-145.
- 499 Balan, N., Bailey, G. J., Jenkins, B., Rao, P. B., & Moffett, R. J. (1994). Variations of ionospheric ionisation and
500 related solar fluxes during an intense solar cycle. *Journal of Geophysical Research: Space Physics*, 99 (A2),
501 2243-2253.
- 502 Balan, N., Bailey, G. J., & Su, Y. Z. (1996). Variations of the ionosphere and related solar fluxes during solar cycles
503 21 and 22. *Advances in Space Research*, 18(3), 11-14.
- 504 Bhuyan, P. K., & Hazarika, R. (2013). GPS TEC near the crest of the EIA at 95 E during the ascending half of solar
505 cycle 24 and comparison with IRI simulations. *Advances in Space Research*, 52(7), 1247-1260.

- 506 Bilitza, D. (2000). The importance of EUV indices for the International Reference Ionosphere. *Physics and*
507 *Chemistry of the Earth, Part C: Solar, Terrestrial & Planetary Science*, 25(5-6), 515-521.
- 508 Chakrabarty, D., Bagiya, M. S., Thampi, S. V., & Iyer, K. N. (2012). Solar EUV flux (0.1-50 nm), F10.7 cm flux,
509 sunspot number and the total electron content in the crest region of equatorial ionisation anomaly during the deep
510 minimum between solar cycle 23 and 24. *94.20. dt; 96.60. qd; 96.60. tj*.
- 511 Chakraborty, S. K., & Hajra, R. (2008). Solar control of ambient ionisation of the ionosphere near the crest of the
512 equatorial anomaly in the Indian zone. *Annales Geophysicae*, 26(1), 47-57.
- 513 Chauhan, V., Singh, O. P., & Singh, B. (2011). Diurnal and seasonal variation of GPS-TEC during a low solar
514 activity period as observed at a low latitude station Agra. *94.20. dv; 96.60. qd*.
- 515 Chen, Y., Liu, L., & Le, H. (2008). Solar activity variations of nighttime ionospheric peak electron density. *Journal*
516 *of Geophysical Research: Space Physics*, 113 (A11).
- 517 Chen, Z., Zhang, S.-R., Coster, A. J., & Fang, G. (2015). EOF analysis and modelling of GPS TEC climatology over
518 North America. *Journal of Geophysical Research: Space Physics*, 120(4), 3118-3129.
- 519 De Abreu, A. J., Fagundes, P. R., Gende, M., Bolaji, O. S., De Jesus, R., & Brunini, C. (2014). Investigation of
520 ionospheric response to two moderate geomagnetic storms using GPS-TEC measurements in the South American
521 and African sectors during the ascending phase of solar cycle 24. *Advances in Space Research*, 53(9), 1313-1328.
- 522 de Adler, N. O., Elías, A. G., & Manzano, J. R. (1997). Solar cycle length variation: Its relation with ionospheric
523 parameters. *Journal of Atmospheric and Solar-Terrestrial Physics*, 59(2), 159-162.
- 524 D'ujanga, F. M., Baki, P., Olwendo, J. O., & Twinamasiko, B. F. (2013). Total electron content of the ionosphere at
525 two stations in East Africa during the 24–25 October 2011 geomagnetic storm. *Advances in Space Research*, 51(5),
526 712-721.
- 527 D'ujanga, F. M., Mubiru, J., Twinamasiko, B. F., Basalirwa, C., & Ssenyonga, T. J. (2012). Total electron content
528 variations in equatorial anomaly region. *Advances in space research*, 50(4), 441-449.
- 529 D'ujanga, F. M., Opio, P., & Twinomugisha, F. (2016). Variation of the total electron content with solar activity
530 during the ascending phase of solar cycle 24 observed at Makerere University, Kampala. *Ionospheric space*
531 *weather: longitude and hemispheric dependences and lower atmosphere forcing*, 145-154.
- 532 Fayose, R. S., Babatunde, R., Oladosu, O., & Groves, K. (2012). Variation of Total Electron Content [TEC] and
533 their effect on GNSS over Akure, Nigeria. *Applied Physics Research*, 4(2), 105.
- 534 Galav, P., Dashora, N., Sharma, S., & Pandey, R. (2010). Characterisation of low latitude GPS-TEC during very low
535 solar activity phase. *Journal of Atmospheric and Solar-Terrestrial Physics*, 72(17), 1309-1317.
- 536 Gorney, D. J. (1990). Solar cycle effects on the near--*Reviews of Geophysics*, 28(3), 315-336.
- 537 Gupta, J. K., & Singh, L. (2000). Long-term ionospheric electron content variations over Delhi. *Annales*
538 *Geophysicae*, 18(12), 1635-1644.
- 539 Hazarika, R., & Bhuyan, P. K. (2014). Spatial distribution of TEC across India in 2005: Seasonal asymmetries and
540 IRI prediction. *Advances in Space Research*, 54(9), 1751-1767.
- 541 Hedin, A. E. (1984). Correlations between thermospheric density and temperature, solar EUV flux, and 10.7-
542 *-Journal of Geophysical Research: Space Physics*, 89 (A11), 9828-9834.

- 543 Huo, X. L., Yuan, Y. B., Ou, J. K., Zhang, K. F., & Bailey, G. J. (2009). Monitoring the global-scale winter anomaly
544 of total electron contents using GPS data. *Earth, Planets and Space*, *61*, 1019-1024.
- 545 Jakowski, N., Schlüter, S., & Sardon, E. (1999). Total electron content of the ionosphere during the geomagnetic
546 storm on 10 January 1997. *Journal of Atmospheric and Solar-Terrestrial Physics*, *61*(3-4), 299-307.
- 547 Jonah, O. F., De Paula, E. R., Muella, M., Dutra, S. L. G., Kherani, E. A., Negreti, P. M. de S., & Otsuka, Y. (2015).
548 TEC variation during high and low solar activities over South American sector. *Journal of Atmospheric and Solar-*
549 *Terrestrial Physics*, *135*, 22-35.
- 550 Kane, R. P. (1980). Irregular variations in the global distribution of total electron content. *Radio Science*, *15*(04),
551 837-842.
- 552 Kane, R. P. (2003). Solar EUV and ionospheric parameters: A brief assessment. *Advances in Space Research*, *32*(9),
553 1713-1718.
- 554 Karia, S. P., & Pathak, K. N. (2011). GPS-based TEC measurements for a period August 2008–December 2009 near
555 the northern crest of Indian equatorial ionospheric anomaly region. *Journal of Earth System Science*, *120*, 851-858.
- 556 Kassa, T., Tilahun, S., & Damtie, B. (2017). Solar activity indices as a proxy for the variation of ionospheric total
557 electron content (TEC) over Bahir dar, Ethiopia during the year 2010–2014. *Advances in Space Research*, *60*(6),
558 1237-1248.
- 559 Kumar, S., & Singh, A. K. (2009). Variation of ionospheric total electron content in Indian low latitude region of the
560 equatorial anomaly during May 2007–April 2008. *Advances in Space Research*, *43*(10), 1555-1562.
- 561 Kumar, S., Singh, A. K., & Lee, J. (2014). Equatorial Ionospheric Anomaly (EIA) and comparison with IRI model
562 during descending phase of solar activity (2005–2009). *Advances in Space Research*, *53*(5), 724-733.
- 563 Kutiev, I. S., Marinov, P. G., & Watanabe, S. (2006). Model of topside ionosphere scale height based on topside
564 sounder data. *Advances in Space Research*, *37*(5), 943-950.
- 565 Legrand, J., & Simon, P. (1989). *Solar cycle and geomagnetic activity: A review for geophysicists. Part I. The*
566 *contributions to geomagnetic activity*. *7*(6), 565-578.
- 567 Lei, J., Liu, L., Wan, W., & Zhang, S.-R. (2005). Variations of electron density based on long-term incoherent
568 scatter radar and ionosonde measurements over Millstone Hill. *Radio science*, *40*(2), 1-10.
- 569 Li, S., Zhou, H., Xu, J., Wang, Z., Li, L., & Zheng, Y. (2019). Modelling and analysis of ionosphere TEC over
570 China and adjacent areas based on EOF method. *Advances in Space Research*, *64*(2), 400-414.
- 571 Lin, C. H., Liu, J. Y., Fang, T.-W., Chang, P. Y., Tsai, H. F., Chen, C. H., & Hsiao, C. C. (2007). Motions of the
572 equatorial ionisation anomaly crests imaged by FORMOSAT--*Geophysical Research Letters*, *34*(19).
- 573 Liu, G., Huang, W., Gong, J., & Shen, H. (2013). Seasonal variability of GPS-VTEC and model during low solar
574 activity period (2006–2007) near the equatorial ionisation anomaly crest location in Chinese zone. *Advances in*
575 *Space Research*, *51*(3), 366-376.
- 576 Liu, H., Stolle, C., Förster, M., & Watanabe, S. (2007). Solar activity dependence of the electron density in the
577 equatorial anomaly regions observed by CHAMP. *Journal of Geophysical Research: Space Physics*, *112* (A11).

578 Liu, J. Y., Chen, Y. I., & Lin, J. S. (2003). Statistical investigation of the saturation effect in the ionospheric foF2
579 versus sunspot, solar radio noise, and solar EUV radiation. *Journal of Geophysical Research: Space Physics*, 108
580 (A2).

581 Liu, L., & Chen, Y. (2009). Statistical analysis on the solar activity variations of the TEC derived at JPL from global
582 GPS observations. *J. Geophys. Res*, 114

583 Liu, L., Wan, W., & Ning, B. (2004). Statistical modelling of ionospheric foF2 over Wuhan. *Radio Science*, 39(2),
584 1-10.

585 Liu, L., Wan, W., Ning, B., Pirog, O. M., & Kurkin, V. I. (2006). Solar activity variations of the ionospheric peak
586 electron density. *Journal of Geophysical Research: Space Physics*, 111 (A8).

587 Morozova, A. L., Ribeiro, P., Blanco, J. J., & Barlyaeva, T. V. (2020). Temperature and pressure variability in mid-
588 latitude low atmosphere and stratosphere-ionosphere coupling. *Advances in Space Research*, 65(9), 2184-2202.

589 Mukherjee, S., Sarkar, S., Purohit, P. K., & Gwal, A. K. (2010). Seasonal variation of total electron content at crest
590 of equatorial anomaly station during low solar activity conditions. *Advances in Space Research*, 46(3), 291-295.

591 Natali, M. P., & Meza, A. (2011). Annual and semiannual variations of vertical total electron content during high
592 solar activity based on GPS observations. *Annales Geophysicae*, 29(5), 865-873.

593 Olwendo, O. J., Baki, P., Cilliers, P. J., Mito, C., & Doherty, P. (2013). Comparison of GPS TEC variations with
594 IRI-2007 TEC prediction at equatorial latitudes during a low solar activity (2009–2011) phase over the Kenyan
595 region. *Advances in Space Research*, 52(10), 1770-1779.

596 Opiyo, P., D'ujanga, F. M., & Ssenyonga, T. (2015). Latitudinal variation of the ionosphere in the African sector
597 using GPS TEC data. *Advances in Space Research*, 55(6), 1640-1650.

598 Oron, S., D'ujanga, F. M., & Ssenyonga, T. J. (2013). *Ionospheric TEC variations during the ascending solar
599 activity phase at an equatorial station, Uganda.*

600 Ouattara, F., & Amory-Mazaudier, C. (2009). Solar–geomagnetic activity and Aa indices toward a standard
601 classification. *Journal of Atmospheric and Solar-Terrestrial Physics*, 71(17-18), 1736-1748.

602 OUATTARA, F., ZOUNDI, C., MAZAUDIÉ, C. A., Fleury, R., & DUCHESNE, P. L. (2011). Determination of
603 total electron content from pseudo distances (Pd) or pseudo range (Pr) at the Koudougou station in Burkina Faso.
604 *Journal des Sciences*, 11, 12-19.

605 Patel, K., Singh, A., Singh, S., & Singh, A. (2019). Causes responsible for intense and severe storms during the
606 declining phase of Solar Cycle 24. *Journal of Astrophysics and Astronomy*, 40(1), 1-9.

607 Patel, N. C., Karia, S. P., & Pathak, K. N. (2017). GPS-TEC variation during low to high solar activity period (2010-
608 2014) under the northern crest of Indian equatorial ionisation anomaly region. *Positioning*, 8(2), 13-35.

609 Paznukhov, V. V., Carrano, C. S., Doherty, P. H., Groves, K. M., Caton, R. G., Valladares, C. E., Seemala, G. K.,
610 Bridgwood, C. T., Adeniyi, J., & Amaeshi, L. L. N. (2012). Equatorial plasma bubbles and L-band scintillations in
611 Africa during solar minimum. *Annales Geophysicae*, 30(4), 675-682.

612 Perevalova, N. P., Polyakova, A. S., & Zalizovski, A. V. (2010). Diurnal variations of the total electron content
613 under quiet helio-geomagnetic conditions. *Journal of Atmospheric and Solar-Terrestrial Physics*, 72(13), 997-1007.

- 614 Perira, F. (2004). *Spatio-temporal analysis of the geomagnetic field and solar acceleration processes observed in*
615 *radio emissions*.
- 616 Prasad, S., Rao, P. R., Prasad, D., Venkatesh, K., & Niranjana, K. (2012). On the variabilities of the Total Electron
617 Content (TEC) over the Indian low latitude sector. *Advances in Space Research*, 49(5), 898-913.
- 618 Rama Rao, P. V. S., Gopi Krishna, S., Niranjana, K., & Prasad, D. (2006). Temporal and spatial variations in TEC
619 using simultaneous measurements from the Indian GPS network of receivers during the low solar activity period of
620 2004–2005. *Annales Geophysicae*, 24(12), 3279-3292.
- 621 Rama Rao, P. V. S., Gopi Krishna, S., Vara Prasad, J., Prasad, S., Prasad, D., & Niranjana, K. (2009). Geomagnetic
622 storm effects on GPS-based navigation. *Annales Geophysicae*, 27(5), 2101-2110.
- 623 Rao, P. R., Venkatesh, K., Prasad, D., & Niranjana, K. (2013). On the uncertainties in the measurement of absolute
624 (true) TEC over Indian equatorial and low latitude sectors. *Advances in Space Research*, 51(7), 1238-1252.
- 625 Richards, P. G. (2001). Seasonal and solar cycle variations of the ionospheric peak electron density: Comparison of
626 measurement and models. *Journal of Geophysical Research: Space Physics*, 106 (A7), 12803-12819.
- 627 Rishbeth, H., & Garriott, O. K. (1969). Introduction to ionospheric physics. *Introduction to ionospheric physics*.
- 628 Sahai, Y., Becker-Guedes, F., Fagundes, P. R., Lima, W. L. C., Otsuka, Y., Huang, C.-S., Espinoza, E. S., Pi, X., De
629 Abreu, A. J., & Bolzan, M. J. A. (2007). Response of nighttime equatorial and low latitude F-region to the
630 geomagnetic storm of 18 August 2003, in the Brazilian sector. *Advances in Space Research*, 39(8), 1325-1334.
- 631 Sethi, N. K., Goel, M. K., & Mahajan, K. K. (2002). Solar Cycle variations of foF2 from IGY to 1990. *Annales*
632 *Geophysicae*, 20(10), 1677-1685.
- 633 Soicher, H. (1988). Travelling ionospheric disturbances (TIDs) at mid-latitudes: Solar cycle phase dependence.
634 *Radio Science*, 23(03), 283-291.
- 635 Sripathi, S., Kakad, B., & Bhattacharyya, A. (2011). Study of equinoctial asymmetry in the Equatorial Spread F
636 (ESF) irregularities over Indian region using multi--*Journal of Geophysical Research: Space Physics*, 116 (A11).
- 637 Su, Y. Z., Bailey, G. J., & Fukao, S. (1999). Altitude dependencies in the solar activity variations of the ionospheric
638 electron density. *Journal of Geophysical Research: Space Physics*, 104 (A7), 14879-14891.
- 639 Tariku, Y. A. (2015). TEC prediction performance of IRI- 2012 model during a very low and a high solar activity
640 phase over equatorial regions, Uganda. *Journal of Geophysical Research: Space Physics*, 120(7), 5973-5982.
- 641 Torr, M. R., & Torr, D. G. (1973). The seasonal behaviour of the F2 layer of the ionosphere. *Journal of Atmospheric*
642 *and Terrestrial Physics*, 35(12), 2237-2251.
- 643 Tsurutani, B., Mannucci, A., Iijima, B., Abdu, M. A., Sobral, J. H. A., Gonzalez, W., Guarnieri, F., Tsuda, T., Saito,
644 A., & Yumoto, K. (2004). Global dayside ionospheric uplift and enhancement associated with interplanetary electric
645 fields. *Journal of Geophysical Research: Space Physics*, 109 (A8).
- 646 Tsurutani, B. T., Gonzalez, W. D., Gonzalez, A. L., Guarnieri, F. L., Gopalswamy, N., Grande, M., Kamide, Y.,
647 Kasahara, Y., Lu, G., & Mann, I. (2006). Corotating solar wind streams and recurrent geomagnetic activity: A
648 review. *Journal of Geophysical Research: Space Physics*, 111 (A7).
- 649 Venkatesh, K., Fagundes, P. R., Prasad, D. V., Denardini, C. M., De Abreu, A. J., De Jesus, R., & Gende, M.
650 (2015). Day---day---*Journal of Geophysical Research: Space Physics*, 120(10), 9117-9131.

651 Venkatesh, K., Fagundes, P. R., Seemala, G. K., de Jesus, R., de Abreu, A. J., & Pillat, V. G. (2014a). On the
652 performance of the IRI- 2012 and NeQuick2 models during the increasing phase of the unusual 24th solar cycle in
653 the Brazilian equatorial and low--*Journal of Geophysical Research: Space Physics*, 119(6), 5087-5105.

654 Venkatesh, K., Fagundes, P. R., Seemala, G. K., de Jesus, R., de Abreu, A. J., & Pillat, V. G. (2014b). On the
655 performance of the IRI- 2012 and NeQuick2 models during the increasing phase of the unusual 24th solar cycle in
656 the Brazilian equatorial and low--*Journal of Geophysical Research: Space Physics*, 119(6), 5087-5105.

657 Walker, G. O., Ma, J. H. K., & Golton, E. (1994). The equatorial ionospheric anomaly in electron content from solar
658 minimum to solar maximum for South East Asia. *Annales Geophysicae*, 12, 195-209.

659 Zakharenkova, I. E., Cherniak, I. V., Krankowski, A., & Shagimuratov, I. I. (2013). Analysis of electron content
660 variations over Japan during solar minimum: Observations and modelling. *Advances in Space Research*, 52(10),
661 1827-1836.

662 Zerbo, J.-L., Amory Mazaudier, C., Ouattara, F., & Richardson, J. D. (2012). Solar wind and geomagnetism:
663 Toward a standard classification of geomagnetic activity from 1868 to 2009. *Annales Geophysicae*, 30(2), 421-426.

664 Zhang, S.-R., & Holt, J. M. (2007). Ionospheric climatology and variability from long--*Journal of Geophysical*
665 *Research: Space Physics*, 112 (A6).

666 Zhao, B., Wan, W., Liu, L., Mao, T., Ren, Z., Wang, M., & Christensen, A. B. (2007). Features of annual and
667 semiannual variations derived from the global ionospheric maps of total electron content. *Annales Geophysicae*,
668 25(12), 2513-2527.

669 Zoundi, C., Ouattara, F. M., Fleury, R., Amory-Mazaudier, C., & Lassudrie-Duchesne, P. (2012). Seasonal TEC
670 variability in West Africa equatorial anomaly region. *European Journal of Scientific Research*, 77(3), 309-319.

671

672

673